Bioorganic & Medicinal Chemistry Letters 20 (2010) 1500–1503

Contents lists available at ScienceDirect

Bioorganic & Medicinal Chemistry Letters

journal homepage: www.elsevier.com/locate/bmcl

Design, synthesis, and evaluation of indole compounds as novel inhibitors targeting Gp41

Guangyan Zhou [a,*], Dong Wu [a], Evan Hermel [a], Edina Balogh [a], Miriam Gochin [a,b,*]

[a] Department of Basic Sciences, Touro University—California, 1310 Johnson Lane, Mare Island, Vallejo, CA 94592, United States
[b] Department of Pharmaceutical Chemistry, University of California San Francisco, CA 94143, United States

ARTICLE INFO

Article history:
Received 16 November 2009
Revised 15 January 2010
Accepted 20 January 2010
Available online 25 January 2010

Keywords:
HIV
gp41
Small molecule inhibitor
Lead optimization
Indole rings

ABSTRACT

A series of indole ring containing compounds were designed based on the structure of the gp41 complex in the region of the hydrophobic pocket. These compounds were synthesized using a Suzuki Coupling reaction, and evaluated using a fluorescence binding assay and cell–cell fusion assay. The observed inhibition constant of compound **7** was 2.1 μM, and the IC_{50} for cell–cell fusion inhibition was 1.1 μM. Assay data indicated that **7** is a promising lead compound for optimization into an effective low molecular weight fusion inhibitor.

The HIV envelope glycoprotein gp41 plays a key role in the early stage of viral entry. Binding of gp120 to cellular receptors triggers a conformational change of gp41 from a pre-fusogenic form to a fusogenic six-helix bundle (6HB) structure. The conformational transition of gp41 mediates fusion of the HIV-1 membrane with the cell membrane, thereby allowing introduction of the viral genome into the target cell.[1] The core crystal structure of gp41 shows that three helices of N-terminal heptad repeats (NHR) form a central trimeric coiled-coil and three helices of C-terminal heptad repeats (CHR) pack in an anti-parallel configuration into the highly conserved hydrophobic grooves on the surface formed by the NHR.[2,3] In each of the grooves, there is a deep hydrophobic pocket, which is critical for stability of the 6HB and viral fusion.[4]

The hydrophobic pocket on the surface of the internal N-helix trimer is an attractive drug target. Three conserved CHR hydrophobic residues with large side chains, Trp628, Trp631, and Ile635 and a charged Asp632, bind into the pocket, forming specific hydrophobic, hydrogen bond and charged interactions with residues at the base of and lining the pocket (Fig. 1).[5] It was proposed that any chemical entity binding to this cavity of gp41will block six-helix bundle formation, and might have inhibitory activity against HIV-1 entry, preventing virus replication.[4,6] The hydrophobic cavity can accommodate a compound with a molecular weight of 500–600 Da. T-20 (Enfuvirtide®), a 36-amino acid synthetic peptide, was approved by the FDA in 2003 as the first fusion inhibitor for treating HIV/AIDS patients.[7,8] It is believed to interact with the NHR and block six-helix bundle and fusion pore formation.[9,10] T-20 and other peptides have critical limitations as drugs: lack of oral bioavailability and high production cost.[11] Therefore, it is urgent to develop orally available small molecule inhibitors targeting gp41.

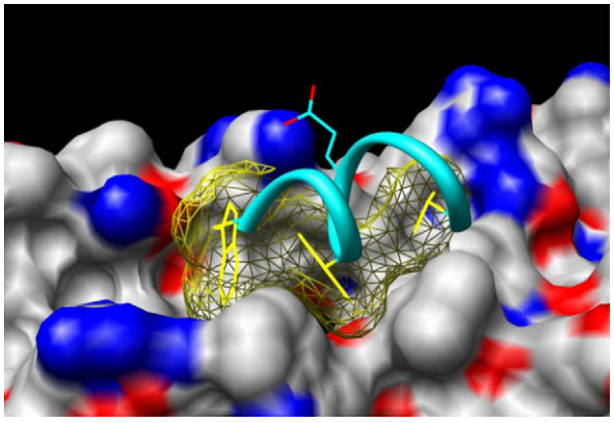

Figure 1. The hydrophobic pocket of gp41 (Molecular dynamics—simulated structure (R. Rizzo, personal communication), starting with PDB 1IF3). The segment of the CHR containing hydrophobic (Trp628, Trp631, and Ile635, in yellow) and charged (Asp632, in cyan) residues is shown interacting in the pocket. Residue numbering is based on Genbank accession number AAK49977.

* Corresponding authors. Tel.: +1 707 638 5482.
E-mail addresses: guangyan.zhou@tu.edu (G. Zhou), miriam.gochin@tu.edu (M. Gochin).

0960-894X/$ - see front matter © 2010 Elsevier Ltd. All rights reserved.
doi:10.1016/j.bmcl.2010.01.111

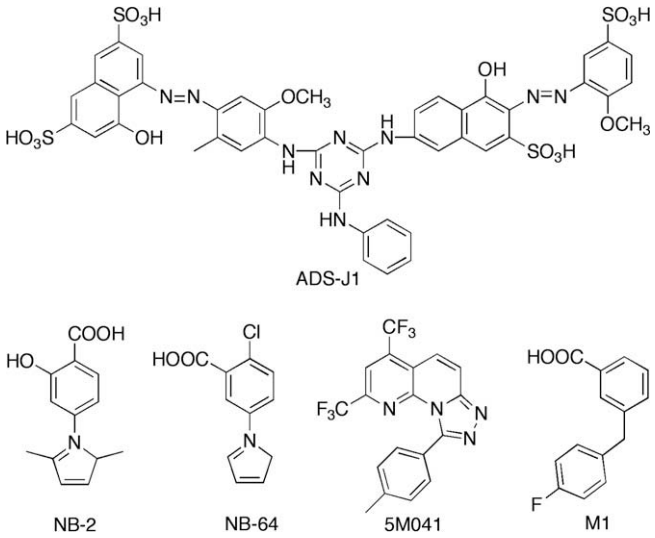

Figure 2. Structures of published gp41 inhibitors proposed to bind in the hydrophobic pocket.

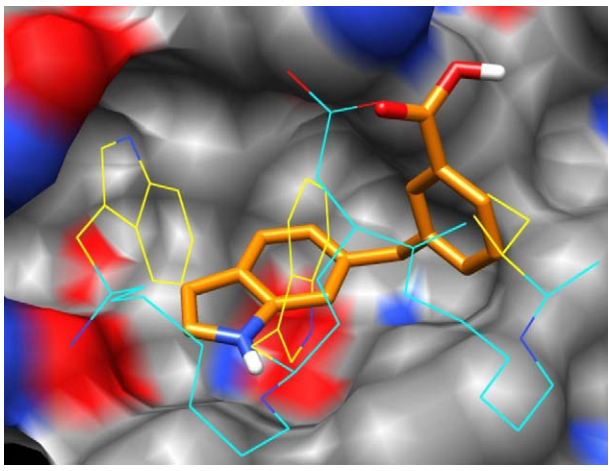

Figure 3. Binding model comparison of **1** (ΔG: −6.6 kcal/mol) and C-peptide (residues 628–635) in the hydrophobic pocket. Compound **1** is shown in orange, the backbone of the C-peptide in cyan. Side chains of the C-peptide are only shown for Trp628, Trp631, Ile635 (in yellow), and Asp632 (in cyan). Heteroatoms are color coded according to standard convention.

Much effort has been devoted towards developing effective small molecular inhibitors targeting this hydrophobic pocket, with limited success. Some inhibitors described as binding in the hydrophobic pocket are shown in Figure 2. They were found by computational or biochemical library screening. The most potent compound found, **ADS-J1**, had an IC_{50} of 0.62 μM against 6HB formation and 4.2 μM against cell–cell fusion (CCF) but is not amenable to modification.[12] Two N-substituted pyrrole derivatives **NB-2** and **NB-64** were identified as anti-HIV agents with IC_{50} values at 7–30 μM levels against CCF in MT-2 cells.[13] Experiments and molecular docking suggested that they bound into the hydrophobic cavity of gp41. They were considered to be leads toward more potent molecules, and some improved activity against CCF was achieved for newly designed compounds based on this scaffold.[13,14] **5M041** was found from a library containing 34,800 compounds, with IC_{50} against CCF of 18 μM.[15] However, no improved activity has been reported.

We have developed a competitive inhibition fluorescence assay for the hydrophobic pocket utilizing a receptor $Fe(env2.0)_3$ and a fluorescently labeled C-peptide.[16] A peptidomimetic library containing 200 compounds was screened, and compound **M1** (Fig. 2) was derived as a weakly active fragment. It has a K_I = 548 μM, CCF IC_{50} = 560 μM. NMR studies demonstrated unequivocally that it bound in the hydrophobic cavity of gp41.[17]

Here, we describe a structure-based approach for discovering small molecule inhibitors of gp41. Based on the NMR structure of the complex of gp41 and **M1**, the indole ring containing compound **1** was designed, and synthesized according to Scheme 1. The design strategy for **1** was to increase ligand hydrophobicity while maintaining solubility by replacing the fluorophenyl group of **M1** with an indole. An indole group on the ligand could possibly emulate the interaction of Trp residues which bind in the pocket in the 6HB structure, and which include a hydrogen bond between the indole NH of Trp631 and the backbone carbonyl of Leu568.[18] Furthermore, it was anticipated that derivatives of **1** would be synthetically feasible due to ease of substitution at the indole and phenyl rings. The binding model of **1** with gp41 was predicted by AutoDock4.0[19,20] and is shown in Figure 3. The salt-bridge between the carbonyl group of **M1** and Lys574.Nε is maintained in the **1** docked structure. A comparison of the binding model of **1** and C-peptide is shown in Figure 3. There is partial overlap of the indole ring of **1** and Trp631. The predicted K_I for binding was 29 μM. The observed binding affinity for **1** was 4.5 μM, considerably improved over both **M1** and a C-peptide comprising just residues 628–635, which has no detectable binding.[21,22] The lack of affinity of the short peptide results from the high entropic penalty of binding of a linear peptide. Compound **1** also showed good activity in inhibition of cell–cell fusion, with an IC_{50} of 3.2 μM.

The compound **1** fits the criteria for selection of a lead compound for optimization: (a) it has a low molecular weight (251.09 Da), (b) it showed good inhibitory activity, and (c) synthetic modifications of the scaffold are possible, particularly at the 1- and 3-positions of the indole heterocycle. Compound **1** is small and does not fill the pocket, suggesting that improved derivatives which include increased hydrophobicity and additional H-bonding may provide the necessary affinity required for a small molecule inhibitor. A series of derivatives of **1** were designed, synthesized and tested in both binding and CCF inhibition. The results are listed in Table 1, and specific data for four of the compounds is shown in Figure 4. Based on the predicted binding model of **1**, there are two Gln side chains (Gln575, Gln577) close to the indole ring that could interact with a ligand to form a hydrogen bond, so polar groups were introduced in compounds **3** and **8** at the 3-position of the indole. To increase the hydrophobicity, compounds **2** and **7**

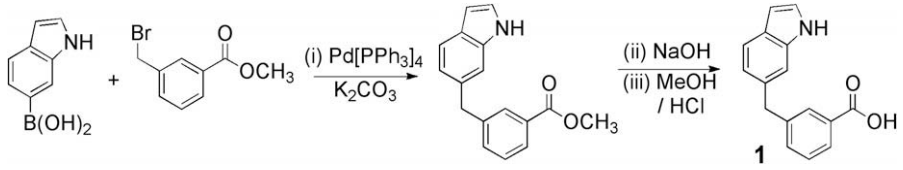

Scheme 1. Synthesis of compound **1** by Suzuki coupling. Reagents and conditions: (i) 5% $Pd(PPh_3)_4$, 2 M K_2CO_3, THF, 80 °C, under N_2, 4h; (ii) 1 M NaOH, CH_3OH/THF(1:4); (iii) 1 M HCl. Overall yield 67%.

Table 1
Activity data: predicted K_I, observed K_I, cell–cell fusion IC_{50} and cytotoxicity CC_{50}, in μM

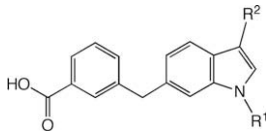

Compound	R^1	R^2	Mol. Wt.	Pred. K_I[a]	Obs. K_I[b]	IC_{50} CCF[c]	CC_{50} cytotoxicity
1	H	H	251.09	29	4.5 ± 0.5	3.2 ± 0.5	>500
2	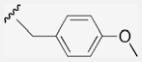	H	371.40	2.3	3.4 ± 0.5	3.7 ± 0.5	100
3	H	–COCOOH	323.30	5.2	393 ± 31	>100	>100
4	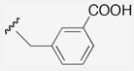	H	385.41	0.43	21.7 ± 1.6	130 ± 5	>200
5	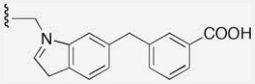	H	514.57	0.41	1.4 ± 0.34	2.9 ± 0.2	80
6	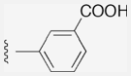	H	371.40	0.59	107 ± 25.4	186 ± 16	>400
7	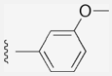	H	357.40	1.3	2.1 ± 0.2	1.1 ± 0.4	>100
8	H	–CHO	279.29	16.5	44.1 ± 1.8	141 ± 59	>100

[a] Predicted K_I of the lowest energy structure, using the pdb structure shown in Figure 1.
[b] Observed inhibition constant by fluorescence assay env2.0/C18-Aib.[16]
[c] Cell–cell fusion assay using HL2/3 and TZM-bl cells.[28]

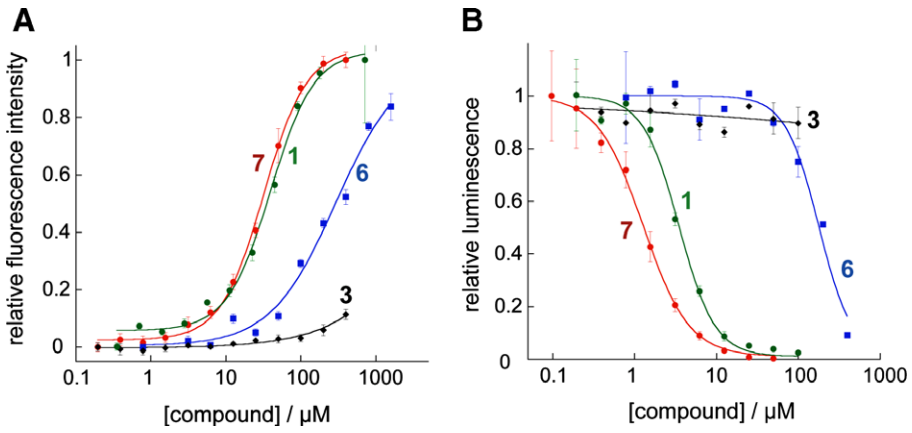

Figure 4. (A) Fluorescence binding analysis and (B) cell–cell fusion of four indole derivatives.

were designed by introducing an aromatic hydrophobic group at the 1-position. The methoxyl group substituent occupies the same location in the pocket in both docked structures. Compounds **4**–**6** contained both increased hydrophobicity and an added carboxylate group. Compounds **4** and **6** differ by a single methylene group, and were synthesized to evaluate entropic and steric effects at this position. The extended inhibitor, **5**, has the highest hydrophobicity. Compounds **6** and **7** were generated by Ullmann reaction[23] using Cu_2O as a catalyst.[24] Compound **5** was synthesized by treating the indole ring with KOH/DMSO, followed by CH_2Cl_2 to form the methylene-bis-1*H*-indole derivative.[25]

There are several noteworthy features of the data in Table 1. Firstly, there was excellent correlation between the observed K_I for binding and the IC_{50} for cell–cell fusion, (correlation coefficient 0.92) suggesting that fusion inhibition was due to binding in the hydrophobic pocket, and the fluorescence assay was an excellent filter for fusion inhibitors against gp41. Secondly, there is reasonable but imperfect agreement between observed K_I and K_I predicted by AutoDock4.0. Increased hydrophobicity improved activity, as predicted, but adding polar groups had a deleterious effect. Calculations which involved carboxylate group interactions with the Gln residues failed to accurately predict observed binding constants. The lack of agreement for these compounds might be caused by the use of a fixed receptor structure of gp41 during the calculation. Flexible docking allowing some flexibility of side chains around the pocket was attempted, but failed to give a main cluster for models of the ligand binding. In addition, electrostatic interaction energies are difficult to compute accurately.[26]

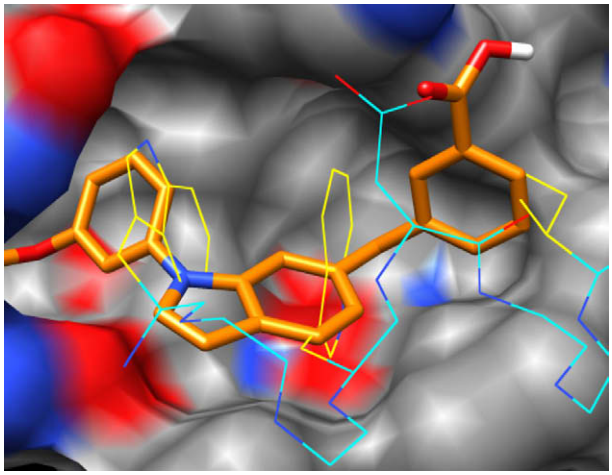

Figure 5. Lowest energy docked structure of **7** in the hydrophobic pocket (ΔG: −7.8 kcal/mol).

The most potent compound in Table 1, **7**, is an example of a modification at the first position of the indole ring.[27] Figure 5 shows the computationally docked orientation and conformation of **7** in the hydrophobic pocket. The salt-bridge distance between the carboxylic acid group of **7** and Lys 574.Nε of gp41 was maintained, and the additional *m*-methoxy-phenyl group provided additional hydrophobic contacts to residues at the bottom of the pocket, occupying the area filled by Trp628 in the 6HB structure. This region was vacant in the docked conformation of **1** (Fig. 3). Compound **7** showed twofold improvement in K_I and threefold improvement in IC_{50} for CCF inhibition over **1**. This compound appears to be more potent than compounds that have been described in the literature so far, and it has been validated as an inhibitor of gp41.

From the initial fragment **M1** to **7**, we have obtained 260-fold improvement in the K_I for binding and 510-fold increased activity against HIV-1 fusion in cell culture. These results validate the use of a rational drug design strategy for development of nonpeptide fusion inhibitors, and suggest future modifications to significantly improve the affinity of small molecules. In summary, our studies demonstrate a series of novel chemical structures as inhibitors against gp41 and establish a solid foundation for future optimization.

Acknowledgments

This work was supported by grant funding from NIH NS059403. The authors acknowledge Dr. Lifeng Cai for advice on new inhibitors targeting gp41. We thank Dr. Shengquan Liu for discussion of the organic synthesis, and Dr. Robert Rizzo at SUNY Stony Brook for providing receptor coordinates. Molecular graphics images were produced using the UCSF Chimera package from the Resource for Biocomputing, Visualization, and Informatics at the University of California, San Francisco (supported by NIH P41 RR-01081).

References and notes

1. Gallo, S. A.; Puri, A.; Blumenthal, R. *Biochemistry* **2001**, *40*, 12231.
2. Caffrey, M.; Cai, M.; Kaufman, J.; Stahl, S. J.; Wingfield, P. T.; Covell, D. G.; Gronenborn, A. M.; Clore, G. M. *EMBO J.* **1998**, *17*, 4572.
3. Chan, D. C.; Fass, D.; Berger, J. M.; Kim, P. S. *Cell* **1997**, *89*, 263.
4. Chan, D. C.; Chutkowski, C. T.; Kim, P. S. *Proc. Natl. Acad. Sci. U.S.A.* **1998**, *95*, 15613.
5. Mo, H.; Konstantinidis, A. K.; Stewart, K.; Dekhtyar, T.; Ng, T.; Swift, K.; Matayoshi, E.; Kati, W.; Kohlbrenner, W.; Molla, A. *Virology* **2004**, *329*, 319.
6. Jiang, S.; Zhao, Q.; Debnath, A. K. *Curr. Pharm. Des.* **2002**, *8*, 563.
7. Kilby, J. M.; Eron, J. J. *N. Engl. J. Med.* **2003**, *348*, 2228.
8. Manfredi, R.; Sabbatani, S. *Curr. Med. Chem.* **2006**, *13*, 2369.
9. Liu, S.; Lu, H.; Niu, J.; Xu, Y.; Wu, S.; Jiang, S. *J. Biol. Chem.* **2005**, *280*, 11259.
10. Naider, F.; Anglister, J. *Curr. Opin. Struct. Biol.* **2009**, *19*, 473.
11. Liu, S.; Wu, S.; Jiang, S. *Curr. Pharm. Des.* **2007**, *13*, 143.
12. Debnath, A. K.; Radigan, L.; Jiang, S. *J. Med. Chem.* **1999**, *42*, 3203.
13. Liu, K.; Lu, H.; Hou, L.; Qi, Z.; Teixeira, C.; Barbault, F.; Fan, B. T.; Liu, S.; Jiang, S.; Xie, L. *J. Med. Chem.* **2008**, *51*, 7843.
14. Wang, Y.; Lu, H.; Zhu, Q.; Jiang, S.; Yun Liao, Y. *Bioorg. Med. Chem. Lett.* **2009**, *Nov 5* [Epub ahead of print].
15. Frey, G.; Rits-Volloch, S.; Zhang, X. Q.; Schooley, R. T.; Chen, B.; Harrison, S. C. *Proc. Natl. Acad. Sci. U.S.A.* **2006**, *103*, 13938.
16. Cai, L.; Gochin, M. *Antimicrob. Agents Chemother.* **2007**, *51*, 2388.
17. Balogh, E.; Wu, D.; Zhou, G.; Gochin, M. *J. Am. Chem. Soc.* **2009**, *131*, 2821.
18. Caffrey, M. *Biochim. Biophys. Acta* **2001**, *1536*, 116.
19. Goodsell, D. S.; Morris, G. M.; Olson, A. J. *J. Mol. Recognit.* **1996**, *9*, 1.
20. Rosenfeld, R. J.; Goodsell, D. S.; Musah, R. A.; Morris, G. M.; Goodin, D. B.; Olson, A. J. *J. Comput. Aided Mol. Des.* **2003**, *17*, 525.
21. Cole, J. L.; Garsky, V. M. *Biochemistry* **2001**, *40*, 5633.
22. Gochin, M.; Cai, L. *J. Med. Chem.* **2009**, *52*, 4338.
23. Fanta, P. E. *Synthesis* **1974**, *1974*, 9.
24. Amamoto, T.; Kurata, Y. *Can. J. Chem.* **1983**, *61*, 86.
25. Kren, V.; Fiserova, A.; Weignerova, L.; Stibor, I.; Halada, P.; Prikrylova, V.; Sedmera, P.; Pospisil, M. *Bioorg. Med. Chem.* **2002**, *10*, 415.
26. Koehl, P. *Curr. Opin. Struct. Biol.* **2006**, *16*, 142.
27. Compound **7** was purified by HPLC using acetonitrile/water as solvents. Mass calculated for $C_{23}H_{19}NO_3$: 357.40; LC–MS: 358.41 (M+1). ^{1}H NMR (400 MHz, DMSO-d_6) δ ppm: 7.81 (1H, s), 7.74 (1H, d, J = 6.8 Hz), 7.61 (1H, d, J = 3.9.8 Hz), 7.58 (1H, d, J = 7.8 Hz), 7.47–7.52 (3H, m), 7.39 (1H, t, J = 6.8 Hz), 7.14 (1H, d, J = 7.8 Hz), 7.08 (1H, s), 7.01 (1H, d, J = 7.8 Hz), 6.96 (1H, d, J = 7.8 Hz), 6.64 (1H, d, J = 2.9 Hz), 4.12 (2H, s), 3.82 (3H, s).
28. Wexler-Cohen, Y.; Shai, Y. *FASEB J.* **2007**, *21*, 3677.